Supporting information

Thermoswitchable Catalysis to Inhibit and Promote Plastic Flow in Vitrimers

Filip Van Lijsebetten,[a] Stephan Maes,[a] Johan M. Winne[a] and Filip E. Du Prez*[a]*

[a] *Polymer Chemistry Research group, Centre of Macromolecular Chemistry (CMaC) and Laboratory of Organic Synthesis, Department of Organic and Macromolecular Chemistry, Faculty of Sciences, Ghent University, Krijgslaan 281-S4, Ghent, 9000, Belgium.*

E-mail: Filip.DuPrez@UGent.be; Johan.Winne@UGent.be

Experimental section

Materials. Materials are trimethylolpropane (97 %, Sigma Aldrich), tert-butyl acetoacetate (TBAA, > 98 %, TCI Europe), tetrahydrofuran (THF, > 99.8 %, Acros Organics), $CDCl_3$ (Euriso-top), trifluoromethane sulfonic acid (> 99%, Sigma Aldrich), acetic acid (> 99%, Chem-Lab Analytical), benzoic acid (99.5%, Sigma Aldrich), 4-nitrobenzoic acid (98%, Sigma-Aldrich),p-toluic acid (98%, Sigma Aldrich), 4-(dimethylamino)benzoic acid (98%, TCI Europe), hexanoic acid (> 99.5 %, Sigma Aldrich), cyclohexane carboxylic acid (98%, Sigma Aldrich), 1-adamantanecarboxylic acid (99%, Sigma Aldrich), Jeffamine D400 was kindly provided by Huntsman, Priamine 1074 was kindly provided by Croda. All reagents were used without further purification unless stated otherwise.

Instrumentation. Nuclear magnetic resonance (NMR) analyses were conducted on a Bruker Avance 300 (300 MHz) to measure proton spectra at 25 °C. The NMR spectra were measured in $CDCl_3$, and chemical shifts (δ) are presented in parts per million (ppm), relative to $CDCl_3$ as the internal standard.

Attenuated total reflection - Fourier-transform infrared spectroscopy (ATR-FTIR) spectra were measured using a Perkin–Elmer Spectrum1000 FTIR infrared spectrometer with a diamond ATR probe.

Thermogravimetric analyses (TGA) were performed with a Mettler Toledo TGA/ SDTA851e instrument under nitrogen atmosphere at a heating rate of 10 $K.min^{-1}$ from 25 °C to 800 °C for the dynamic mode. Isothermal measurements were conducted under air at 160 °C for 120 min. Differential scanning calorimetry (DSC) analyses were performed with a Mettler Toledo instrument 1/700 under nitrogen atmosphere at a heating and cooling rate of 10 $K.min^{-1}$. Measurements were performed from -50 to 150 °C.

A SpeedMixer DAC 150.1 FVZ was used to homogenise the samples before curing.

Rheology experiments were performed on an Anton Paar MCR 302. The experiments were performed in parallel plate geometry using 8 mm sample disks with a thickness of 1 mm. Amplitude sweep experiments were performed using a frequency of 1 Hz, a constant force of 1 N, and a variable shear strain that was ramped up logarithmically from 0.01% to 10%. Stress-relaxation experiments were performed at different temperatures between 160 and 90 °C using a constant shear strain of 0.5 % within the linear viscoelastic region of the samples and a constant force. Each measuring step was preceded by a force normalisation step while monitoring the gap between each plate. Creep experiments were performed between 30 and 80 °C with a 2000 Pa shear stress applied for 5000 s.

Reprocessing. The networks were (re)processed by compression molding. The samples were shredded into small pieces (~1 mm) and put into a mold. The filled mold was put into a heated press at 150 °C for 5 – 10 minutes depending on the flow behaviour of the material, the assembly was pressed at 2 tons. Then the sample was removed from the mold while still hot and in the elastic state.

Solubility. Samples of 4 mm diameter and 2 mm of thickness weighing around 30 mg were submerged in 20 mL of THF in a glass vial. The tests were performed for 24 hours at 25°C after which the solvent was removed and the samples were dried *in vacuo* at 40°C overnight. The soluble fraction and swelling ratio were calculated using **Eq 3** and **Eq 4** respectively, with m_i, m_s, and m_d standing for the initial mass, the swollen mass and the dry mass respectively.

$$soluble\ fraction\ (\%) = \frac{m_i - m_d}{m_i} \quad (3)$$

$$swelling\ ratio\ (\%) = \frac{m_s - m_i}{m_i} \quad (4)$$

Synthetic procedures

1,1,1-Trimethylpropane trisacetoacetate. Trimethylolpropane (10 g, 74.5 mmol, 1 eq.) and tert-butyl acetoacetate (42.44 g, 268.2 mmol, 3.6 eq.) were added in a 250 mL flask equipped with a still-head, a thermometer and a cooler. The viscous mixture was heated to 135 °C until the temperature of the vapour dropped to 40 °C. The unreacted tert-butyl acetoacetate was removed by vacuum distillation at 130 °C under 2 mbar pressure. Yield: 94 % ^{1}H NMR (300 MHz, $CDCl_3$, see **Figure S35**): δ (ppm) = 0.85 (t, *J* = 7.1 Hz, 3H, C**H₃**CH_2C), 1.42 (q, *J* = 7.6 Hz, 2H, CH_3C**H₂**C), 2.21 (s, 9H, 3xC**H₃**$COCH_2$), 3.45 (s, 6H, 3xCH_3COC**H₂**COO), 4.04 (s, 6H, 3xCC**H₂**OCO)

Network synthesis. First the Priamine 1074 (1.575 eq) and acid (0, 4 or 6 mol% with respect to the Priamine 1074) were mixed in a 20 mL polypropylene cup using a DAC 150.1 FVZ speedmixer (typically mixing conditions: 3500 rpm for 2 min) yielding a clear solution. Then trimethylolpropane trisacetoacetate (1 eq) was added and the contents were mixed again. Finally, the cup was transferred to an oven at 80 °C for 4 hours to initiate network formation after which the reaction mixture was further cured in a vacuum oven at 100 °C for 24 hours to ensure complete curing.

Material characterisation

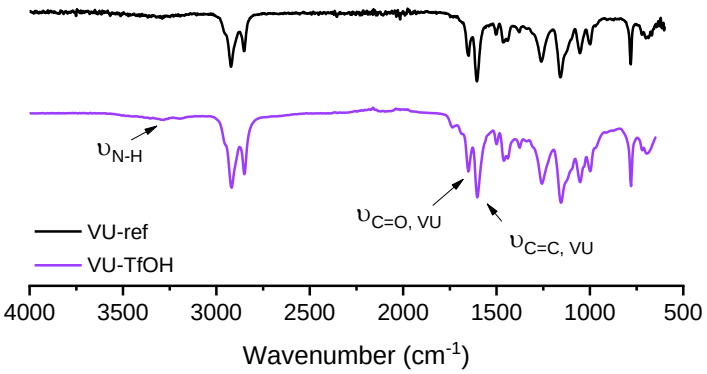

Figure S1. *FT-IR spectrum of VU-ref and VU-TfOH.*

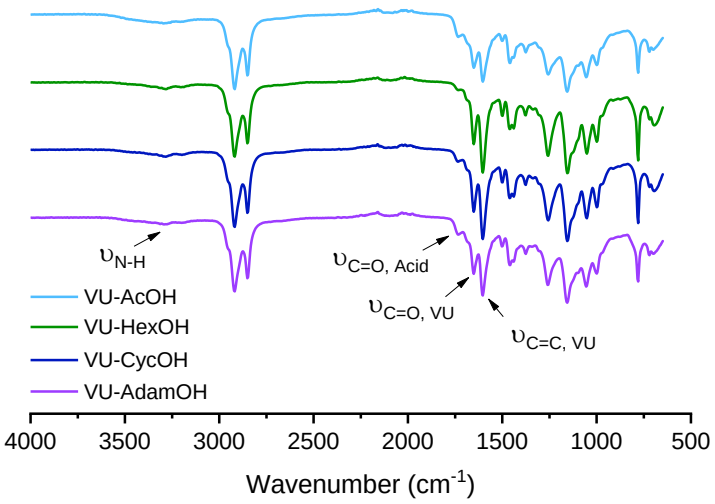

Figure S2. *FT-IR spectrum of VU-AcOH, VU-HexOH, VU-CycOH and VU-AdamOH.*

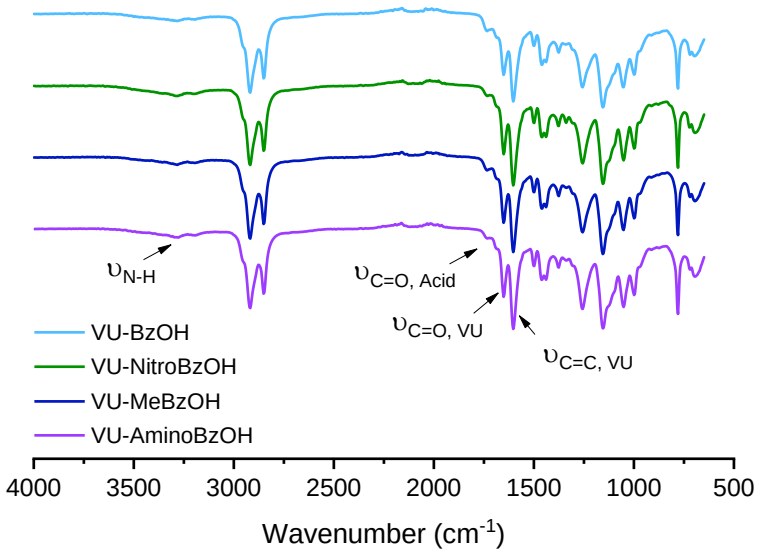

Figure S3. *FT-IR spectrum of VU-BzOH, VU-NitroBzOH, VU- MeBzOH and VU-AminoBzOH.*

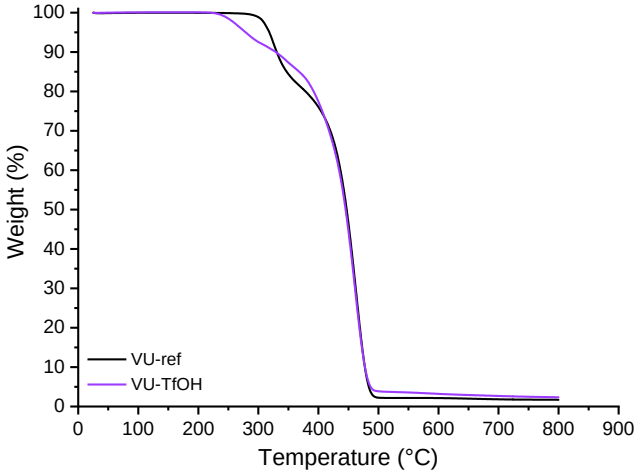

Figure S4. *TGA analysis of VU-ref and VU-TfOH measured under N_2 atmosphere with a temperature ramp from 25-800 °C and a heating rate of 10 °C.min^{-1}.*

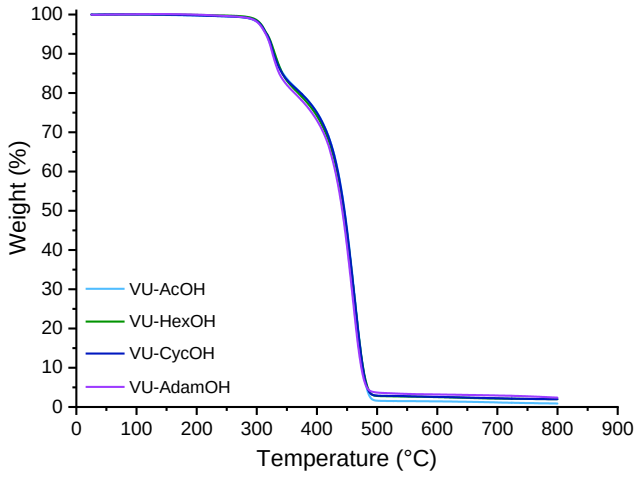

Figure S5. *TGA analysis of VU-AcOH, VU-HexOH, VU-CycOH and VU-AdamOH measured under N_2 atmosphere with a temperature ramp from 25-800 °C and a heating rate of 10 °C.min^{-1}.*

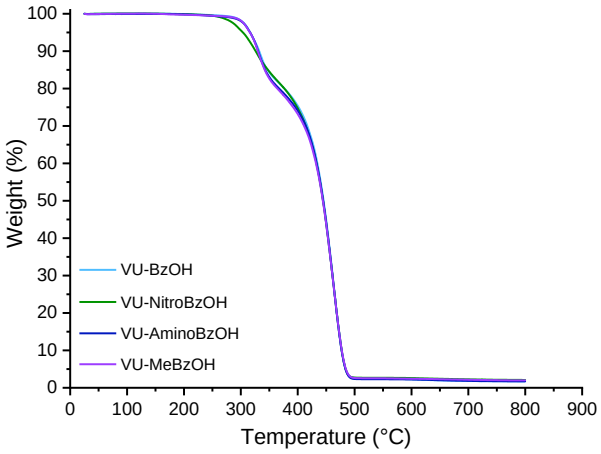

Figure S6. *TGA analysis of VU-BzOH, VU-NitroBzOH, VU- MeBzOH and VU-AminoBzOH measured under N_2 atmosphere with a temperature ramp from 25-800 °C and a heating rate of 10 °C.min^{-1}.*

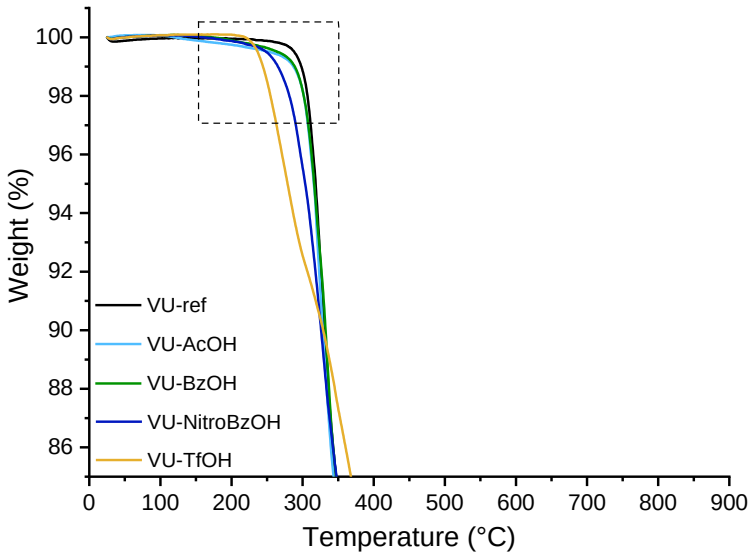

Figure S7. *Spectral zoom of the TGA analysis of VU-ref, VU-AcOH, VU-BzOH, VU-NitroBzOH and VU-TfOH measured under N_2 atmosphere with a temperature ramp from 25-800 °C and a heating rate of 10 °C.min^{-1}. Based on the tendency of acid ionisation, large differences in the onset of thermal degradation can be observed.*

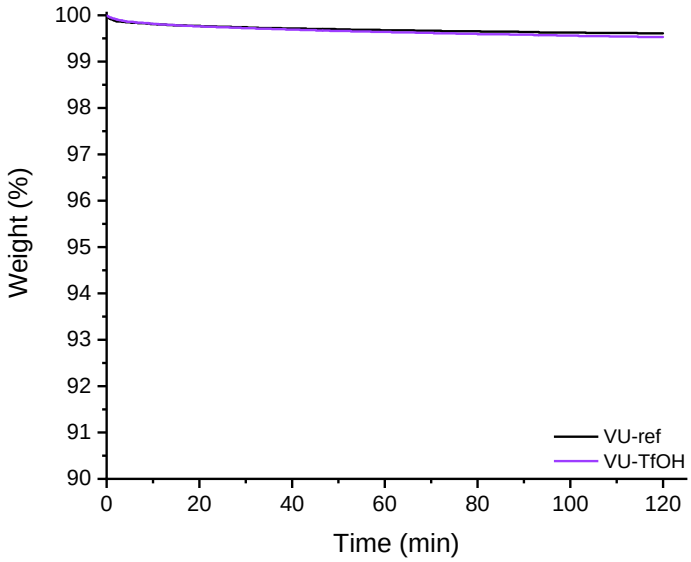

Figure S8. *Isothermal TGA measurements of VU-ref and VU-TfOH at 160 °C for 120 minutes under air.*

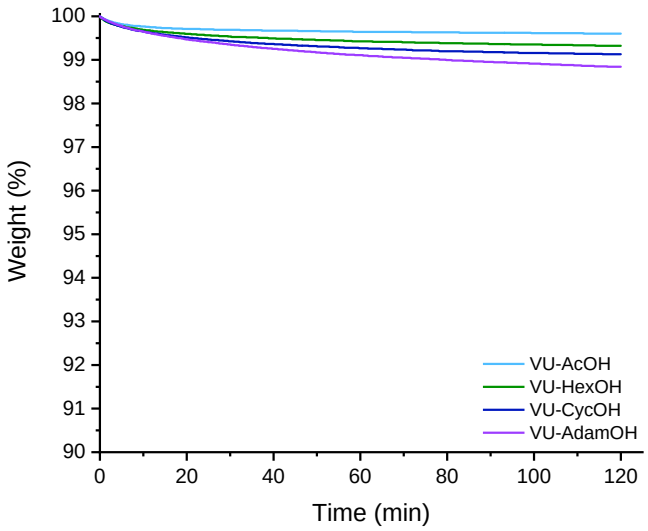

Figure S9. *Isothermal TGA measurements of VU-AcOH, VU-HexOH, VU-CycOH and VU-AdamOH at 160 °C for 120 minutes under air.*

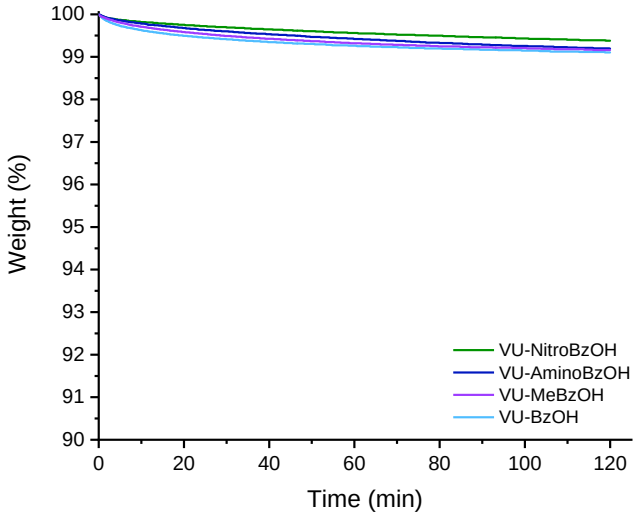

Figure S10. *Isothermal TGA measurements of VU-BzOH, VU-NitroBzOH, VU- MeBzOH and VU-AminoBzOH at 160 °C for 120 minutes under air.*

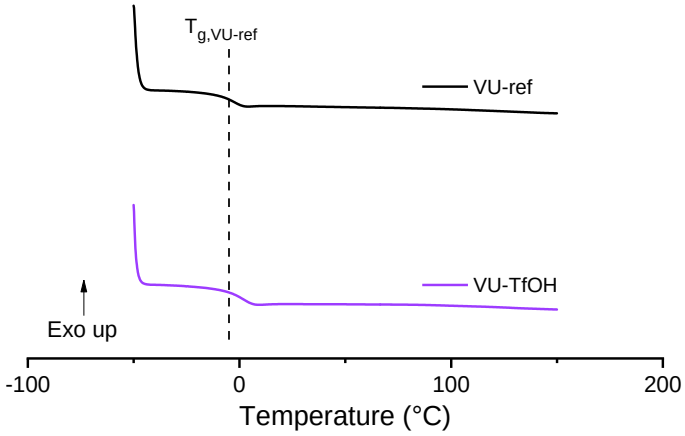

Figure S11. *DSC thermograms of the second heating step of VU-ref and VU-TfOH measured at a heating rate of 10 °C.min^{-1}.*

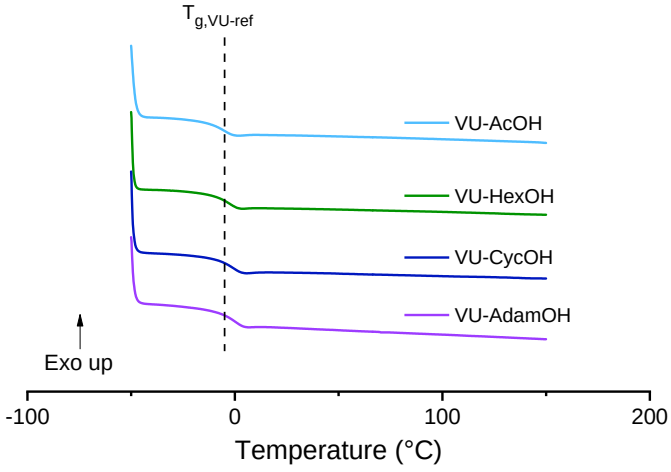

Figure S12. *DSC thermograms of the second heating step of VU-AcOH, VU-HexOH, VU-CycOH and VU-AdamOH measured at a heating rate of 10 °C.min^{-1}.*

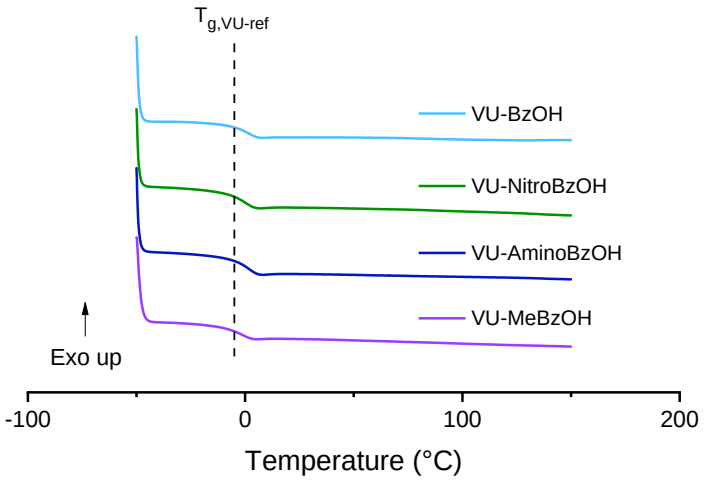

Figure S13. *DSC thermograms of the second heating step of VU-BzOH, VU-NitroBzOH, VU- MeBzOH and VU-AminoBzOH measured at a heating rate of 10 °C.min^{-1}.*

a) VU-ref b) VU-TfOH

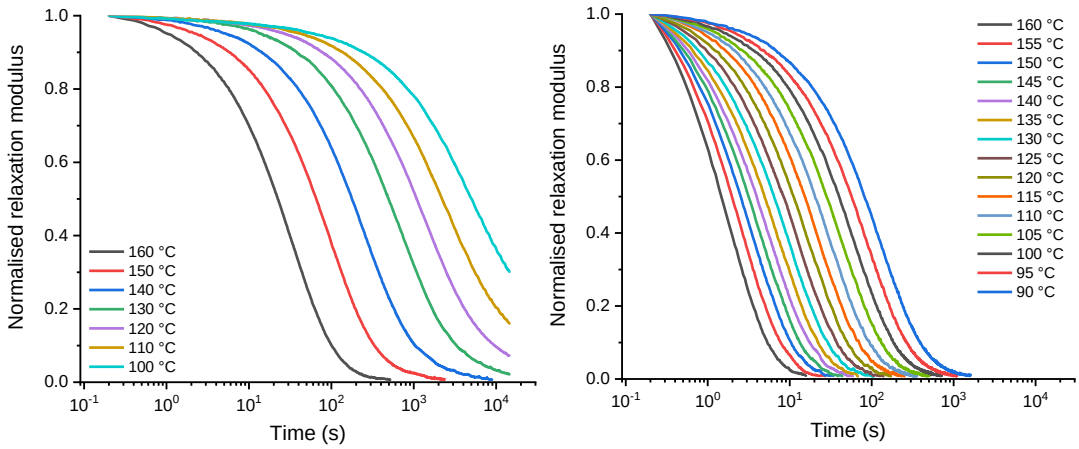

Figure S14. *Normalised stress-relaxation graphs for a) VU-ref and b) VU-TfOH measured at different temperatures between 160 and 90 °C.*

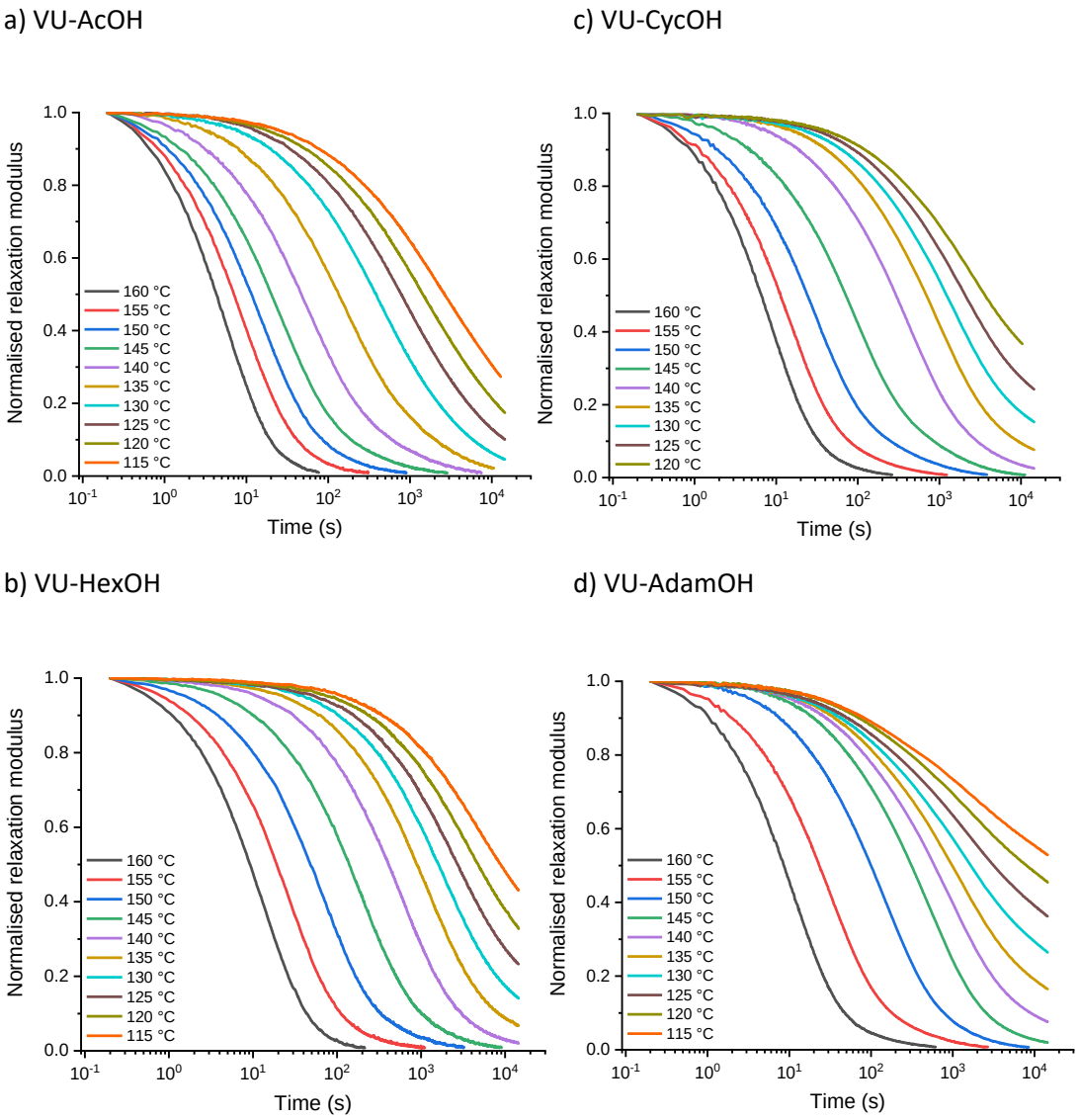

Figure S15. *Normalised stress-relaxation graphs for a) VU-AcOH, b) VU-HexOH, c) VU-CycOH and d) VU-AdamOH measured at different temperatures between 160 and 115 °C.*

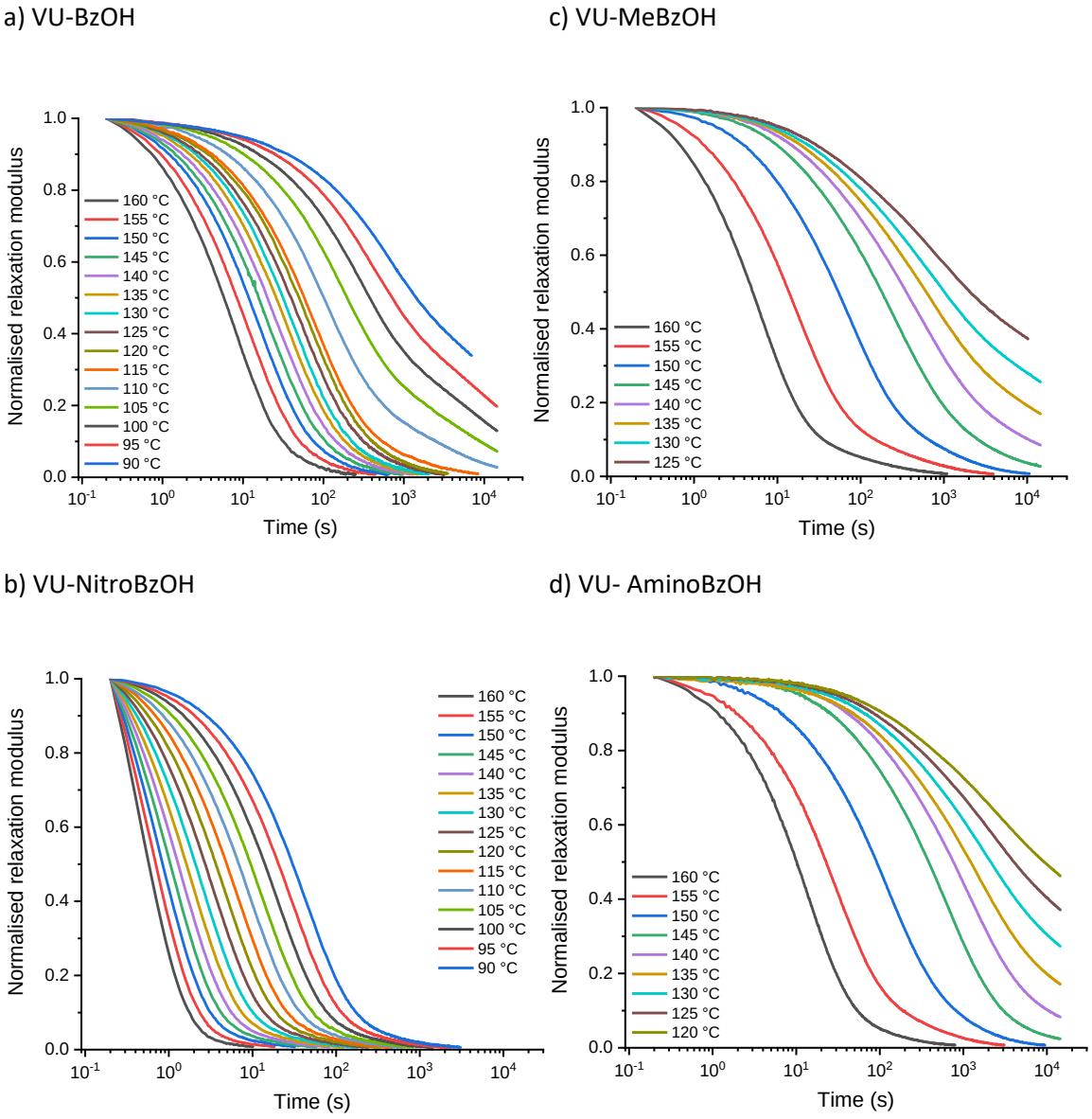

Figure S16. *Normalised stress-relaxation graphs for a) VU-BzOH, b) VU-NitroBzOH, c) VU- MeBzOH and d) VU-AminoBzOH measured at different temperatures between 160 and 90 °C.*

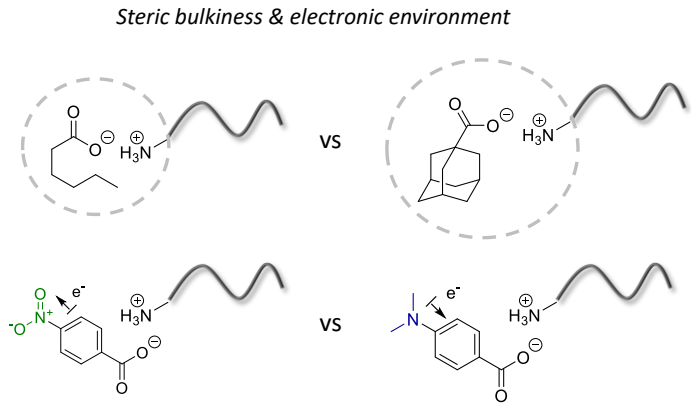

Scheme S1. *Schematic overview of the influence of the Brønsted acid counterion on chain diffusion and the stability of the charged complex.*

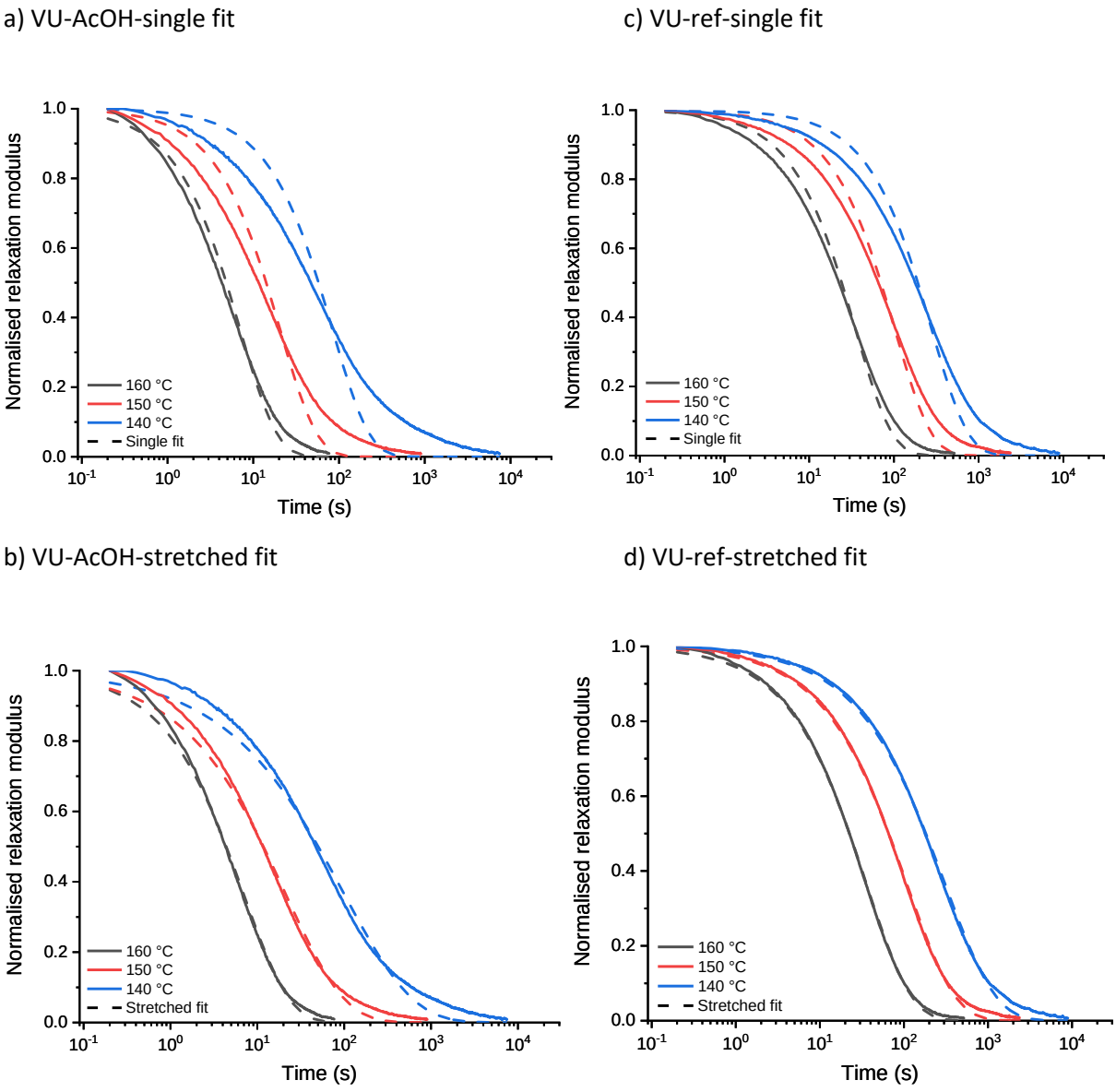

Figure S17. *Normalised stress-relaxation graphs for VU-AcOH with a) a single exponential and b) a stretched exponential fit and for VU-ref with c) a single exponential and d) a stretched exponential fit to the relaxation data from 160 to 140 °C. Especially for VU-AcOH a clear deviation from a single exponential decay could be observed.*

a) VU-MeBzOH-single fit

b) VU-MeBzOH-stretched fit

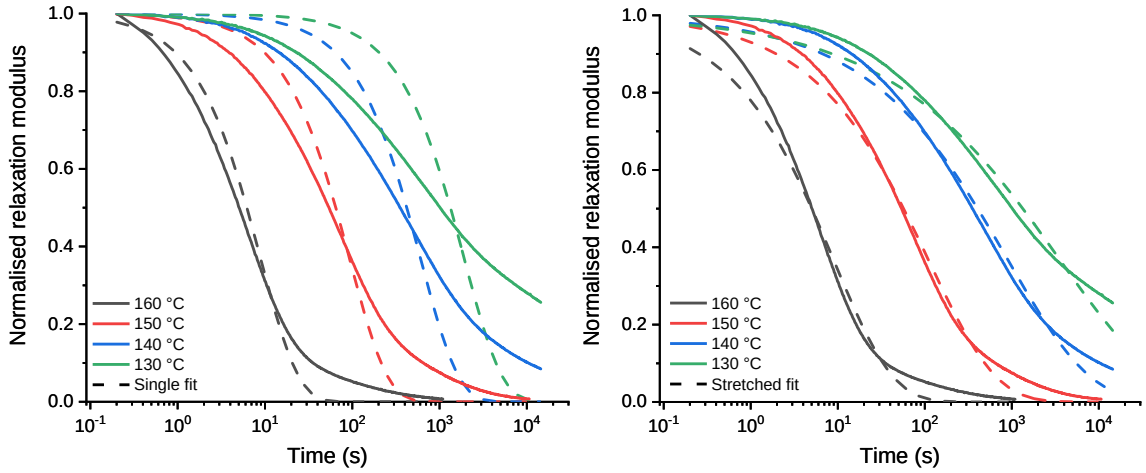

Figure S18. *Normalised stress-relaxation graphs for VU-MeBzOH with a) a single exponential and b) a stretched exponential fit to the relaxation data from 160 to 130 °C. Especially at lower temperatures a clear deviation from a single exponential decay could be observed.*

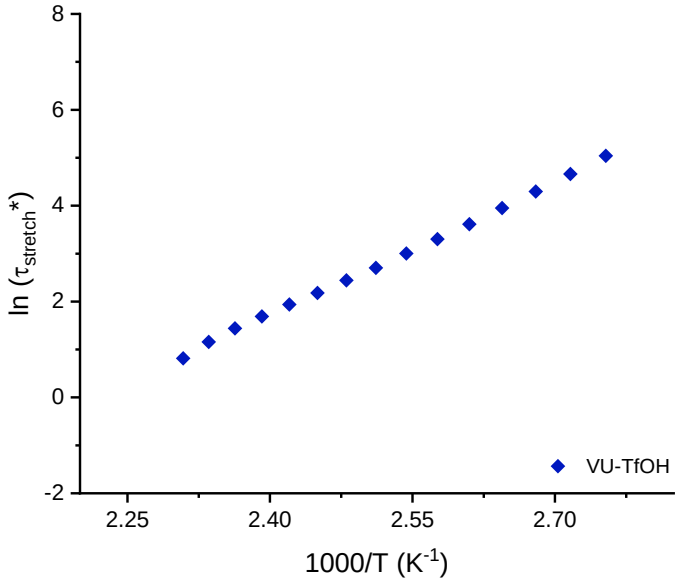

Figure S19. *Arrhenius plot based on relaxation times obtained by a stretched exponential fit to the data of VU-TfOH from 160 to 90 °C.*

a) VU-AcOH-1st recycling step b) VU-AcOH-3rd recycling step

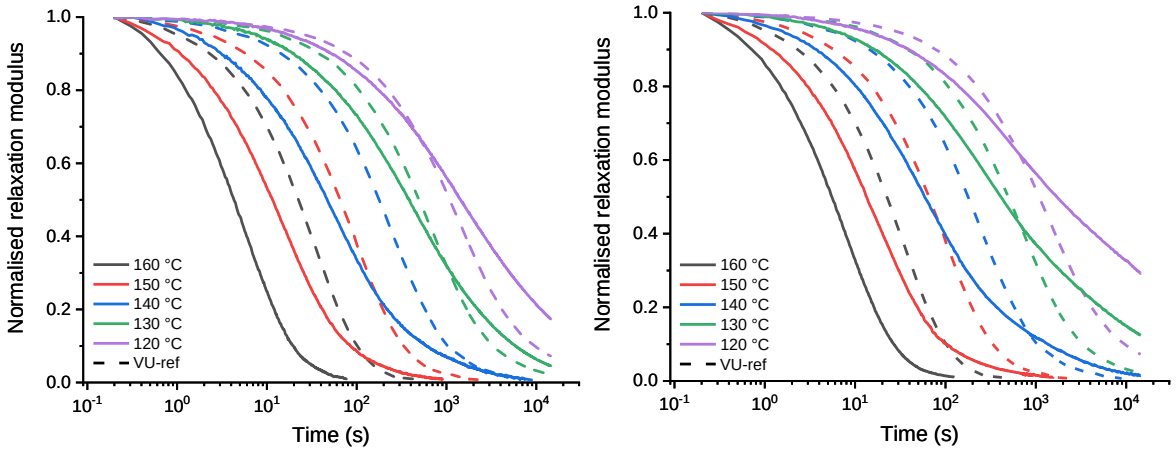

Figure S20. *Normalised stress-relaxation graphs for VU-AcOH when compared to VU-ref from 160 to 120 °C a) after one recycling step and b) after three recycling steps. At lower temperatures, the stress-relaxation measurements may have larger errors for creep-resistant materials.*

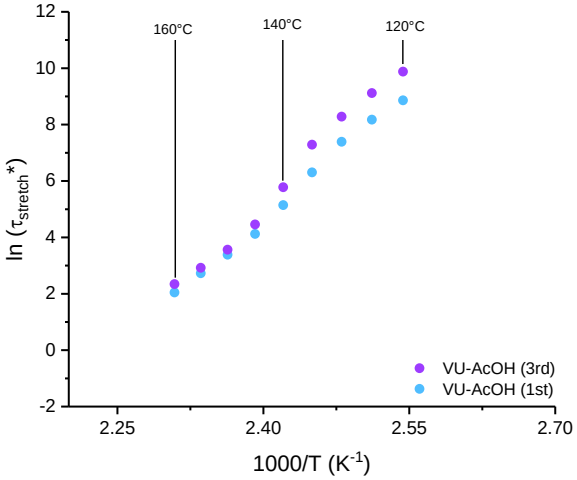

Figure S21. *Arrhenius plot based on relaxation times obtained by a stretched exponential fit to the data of VU-AcOH after a 1st and 3rd recycling step from 160 to 120 °C.*

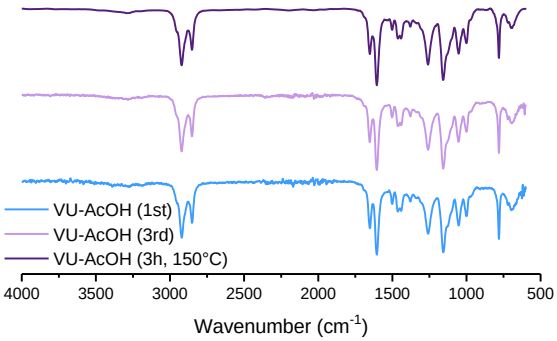

Figure S22. *FT-IR spectrum of VU-AcOH, VU-AcOH after 3 reprocessing cycles and VU-AcOH after heat treatment at 150°C for 3 hours.*

a) VU-AcOH-double fit

b) VU-MeBzOH-double fit

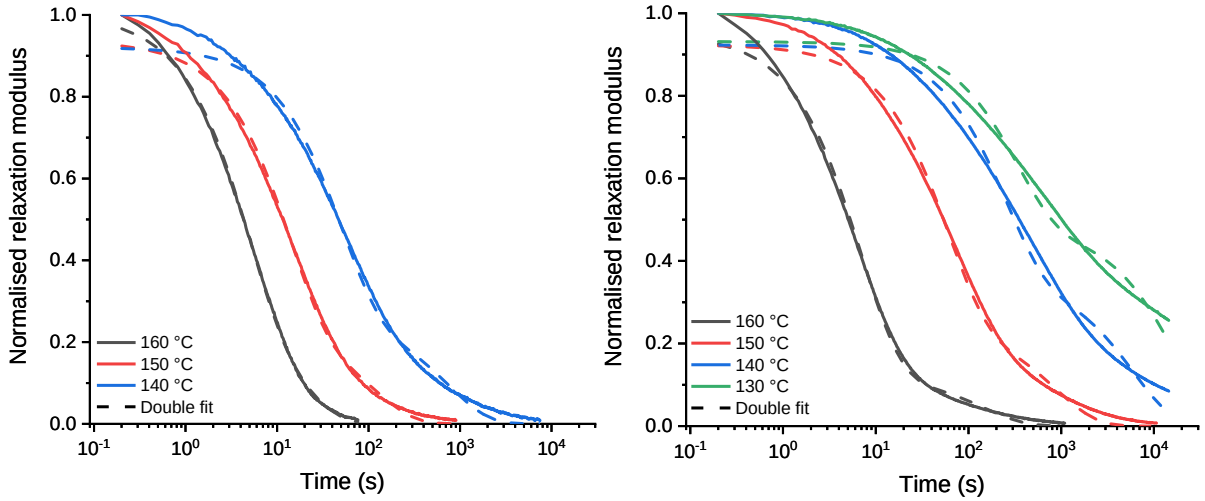

Figure S23. *Normalised stress-relaxation graphs of a) VU-AcOH and b) VU-MeBzOH with a double exponential fit to the data.*

a)

b)

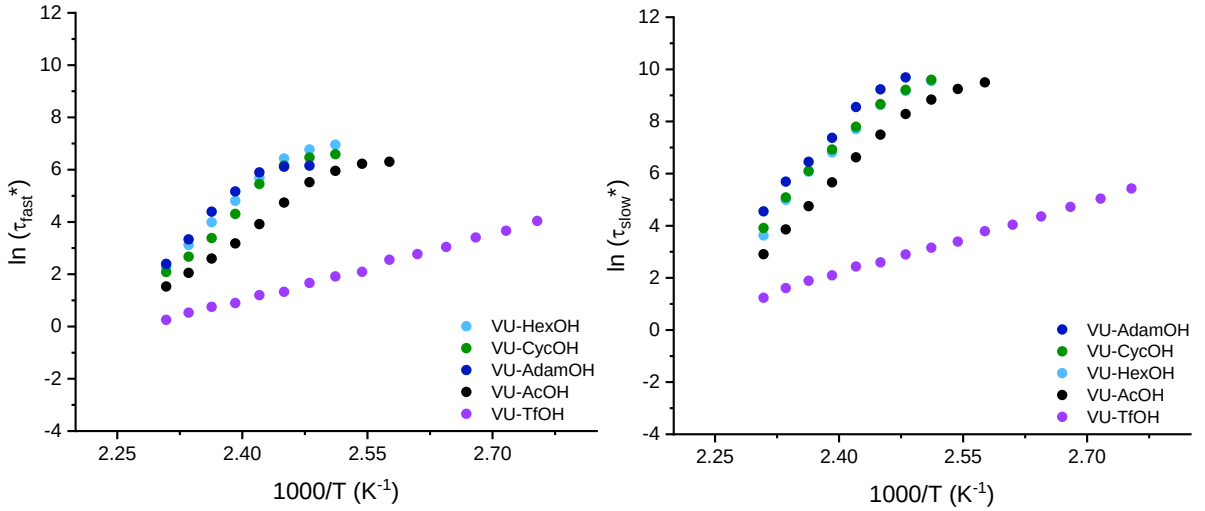

Figure S24. *Arrhenius plot based on relaxation times obtained by a double exponential fit to the data of VU-AcOH, VU-HexOH, VU-CycOH, VU-AdamOH and VU-TfOH with a) the first faster relaxing element and b) the second slower relaxing element.*

a) b)

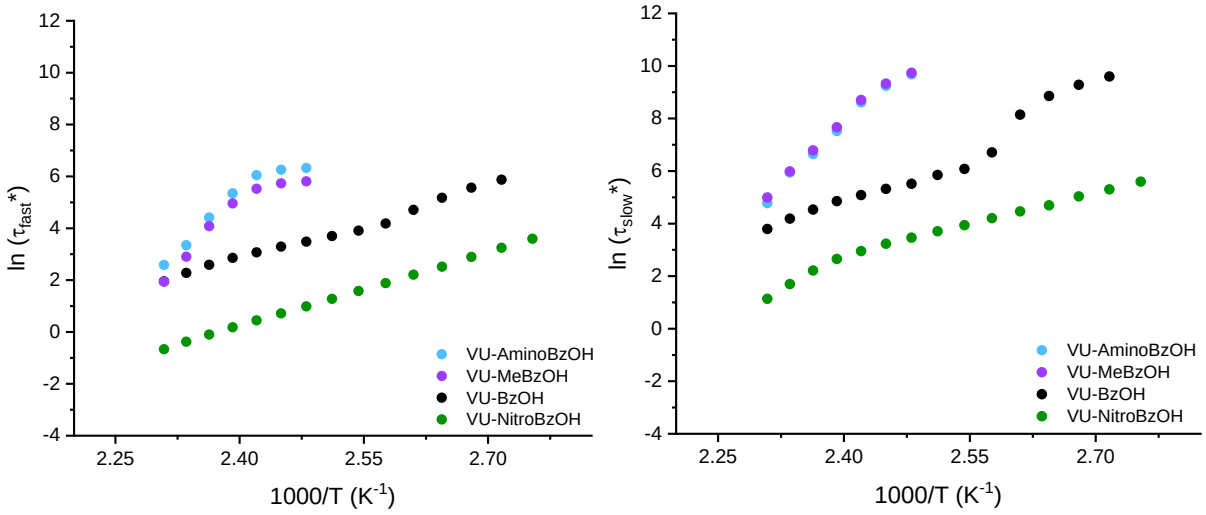

Figure S25. *Arrhenius plot based on relaxation times obtained by a double exponential fit to the data of VU-BzOH, VU-NitroBzOH, VU- MeBzOH and VU-AminoBzOH with a) the first faster relaxing element and b) the second slower relaxing element.*

Table S1. *A double exponential fit to the relaxation data of VU-TfOH, VU-AcOH and VU-BzOH, resulted in two elements (a fast and slow one) with a different weight to the relaxation function G(t).*

Temp	Weight slow element VU-TfOH	Weight fast element VU-TfOH	Weight slow element VU-AcOH	Weight fast element VU-AcOH	Weight slow element VU-BzOH	Weight fast element VU-BzOH
160 °C	**0.40**	**0.60**	**0.30**	**0.70**	**0.25**	**0.75**
150 °C	0.40	0.60	0.35	0.65	0.25	0.75
140 °C	0.40	0.60	0.35	0.65	0.30	0.70
130 °C	0.40	0.60	0.45	0.55	0.30	0.70
115 °C	**0.40**	**0.60**	**0.65**	**0.35**	**0.40**	**0.60**

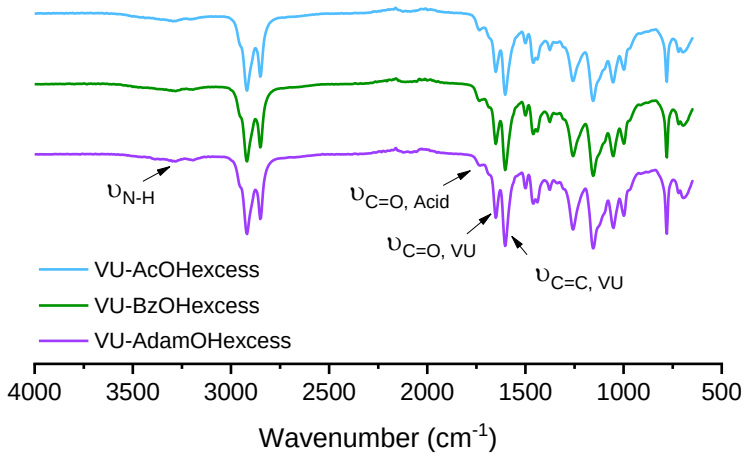

Figure S26. *FT-IR spectrum of VU-AcOHexcess, VU-BzOHexcess and VU-AdamOHexcess.*

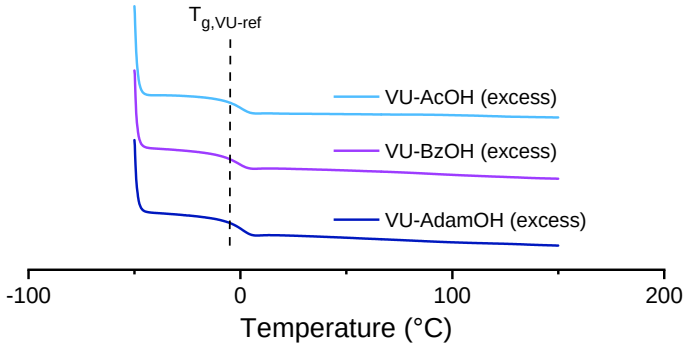

Figure S27. *DSC thermograms of the second heating step of VU-AcOHexcess, VU-BzOHexcess and VU-AdamOHexcess measured at a heating rate of 10 °C.min-1.*

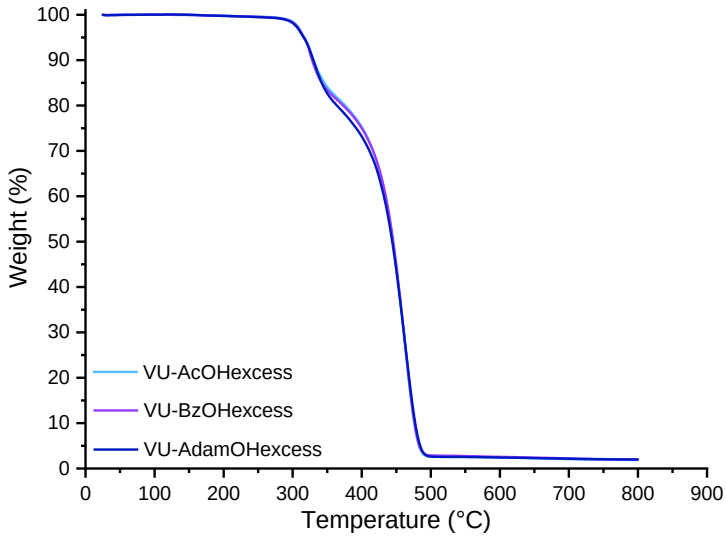

Figure S28. *TGA analysis of VU-AcOHexcess, VU-BzOHexcess and VU-AdamOHexcess measured under a N_2 atmosphere with a temperature ramp from 25-800 °C and a heating rate of 10 °C.min-1.*

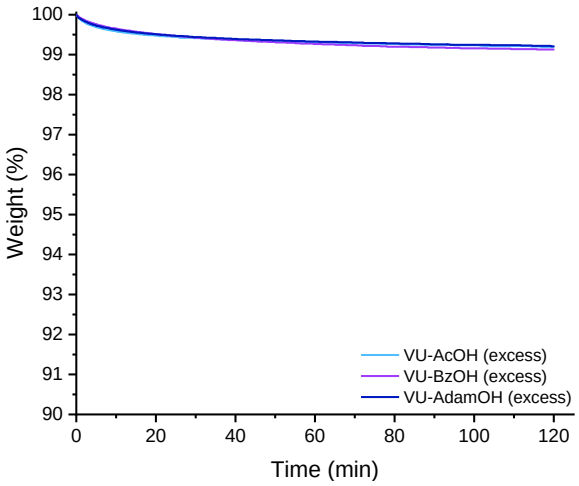

Figure S29. *Isothermal TGA measurements of VU-AcOHexcess, VU-BzOHexcess and VU-AdamOHexcess at 160 °C for 120 minutes under air.*

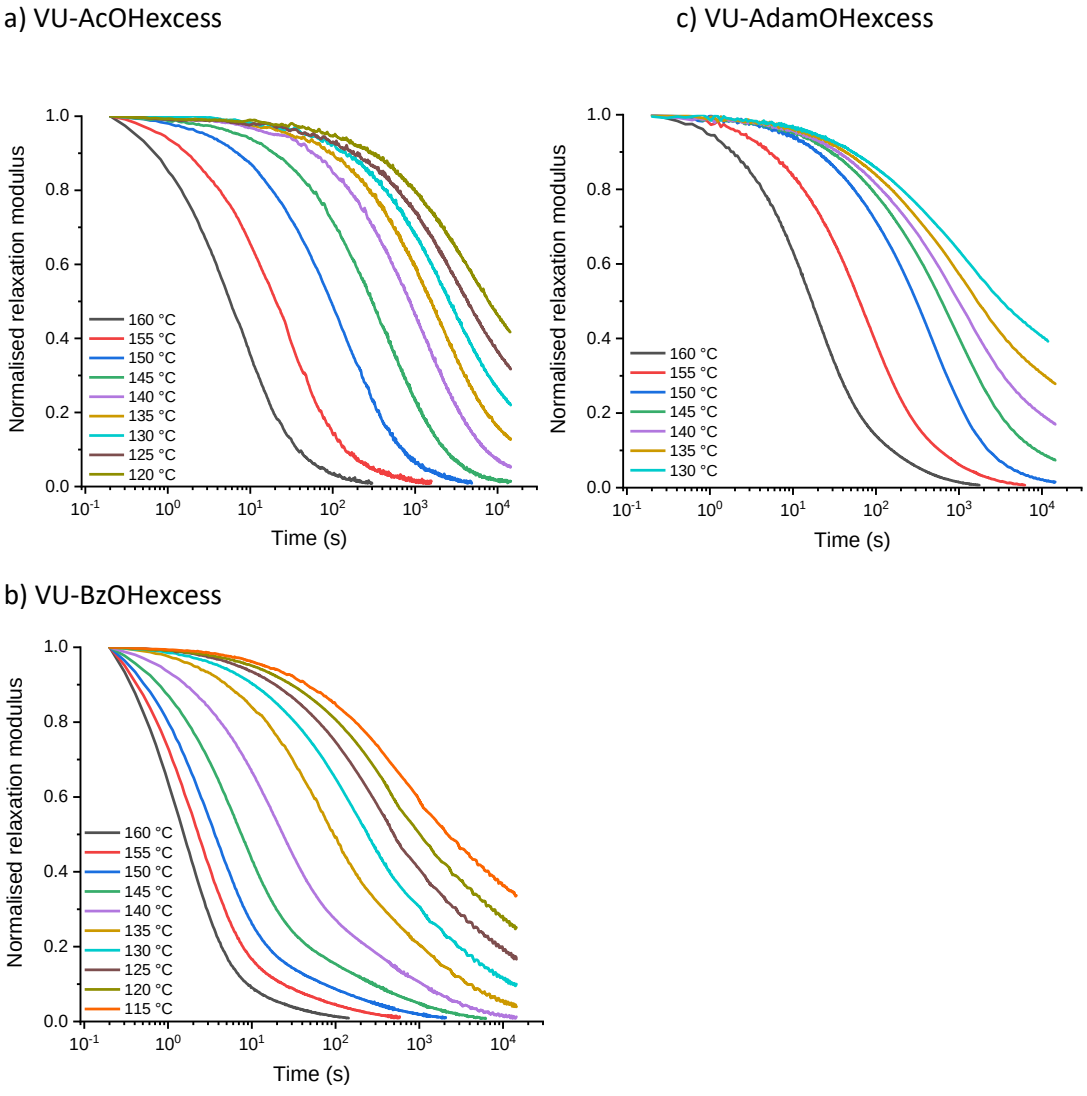

Figure S30. *Normalised stress-relaxation graphs for a) VU-AcOHexcess, b) VU-BzOHexcess and c) VU-AdamOHexcess measured at different temperatures between 160 and 115 °C.*

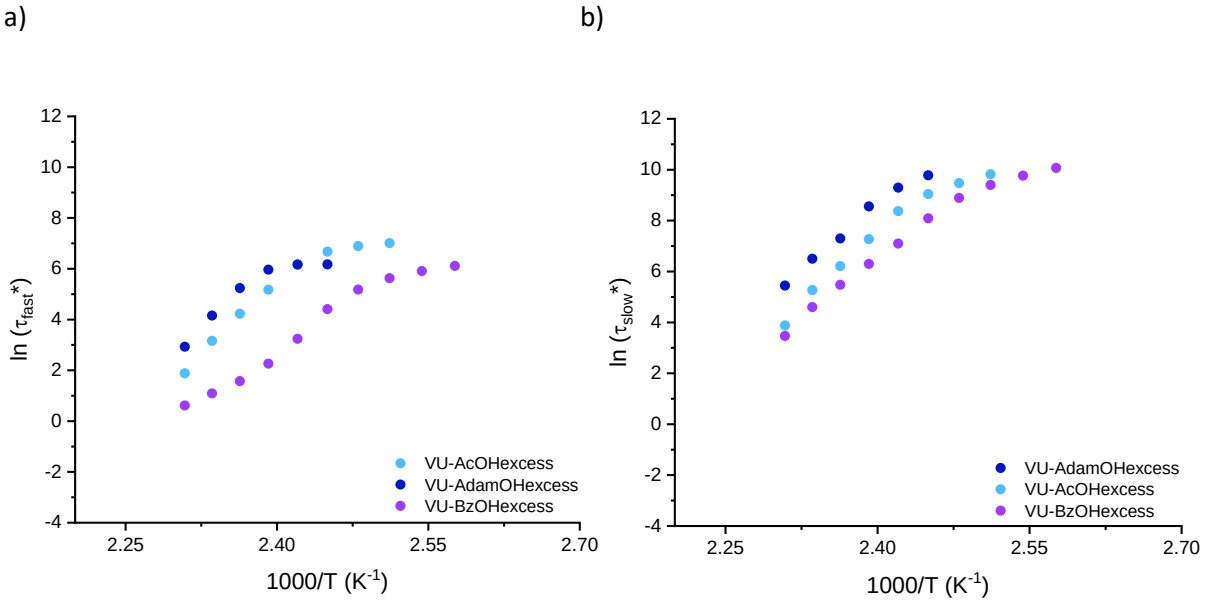

Figure S31. *Arrhenius plot based on relaxation times obtained by a double exponential fit to the data of VU-AcOHexcess, VU-BzOHexcess and VU-AdamOHexcess with a) the first faster relaxing element and b) the second slower relaxing element.*

Table S2. *A double exponential fit to the relaxation data of VU-AcOHexcess, VU-BzOHexcess and VU-AdamOHexcess resulted in two elements (a fast and slow one) with a different weight to the relaxation function G(t).*

Temp	Weight slow element VU-AcOHex	Weight fast element VU-AcOHex	Weight slow element VU-BzOHex	Weight fast element VU-BzOHex	Weight slow element VU-AdamOHex	Weight fast element VU-AdamOHex
160 °C	**0.25**	**0.75**	**0.05**	**0.95**	**0.25**	**0.75**
150 °C	0.45	0.55	0.15	0.85	0.50	0.50
140 °C	0.50	0.50	0.30	0.70	0.55	0.45
130 °C	0.55	0.45	0.35	0.65	**0.65**	**0.35**
120 °C	**0.70**	**0.30**	**0.50**	**0.50**	*	*

* Only measured up to 130 °C.

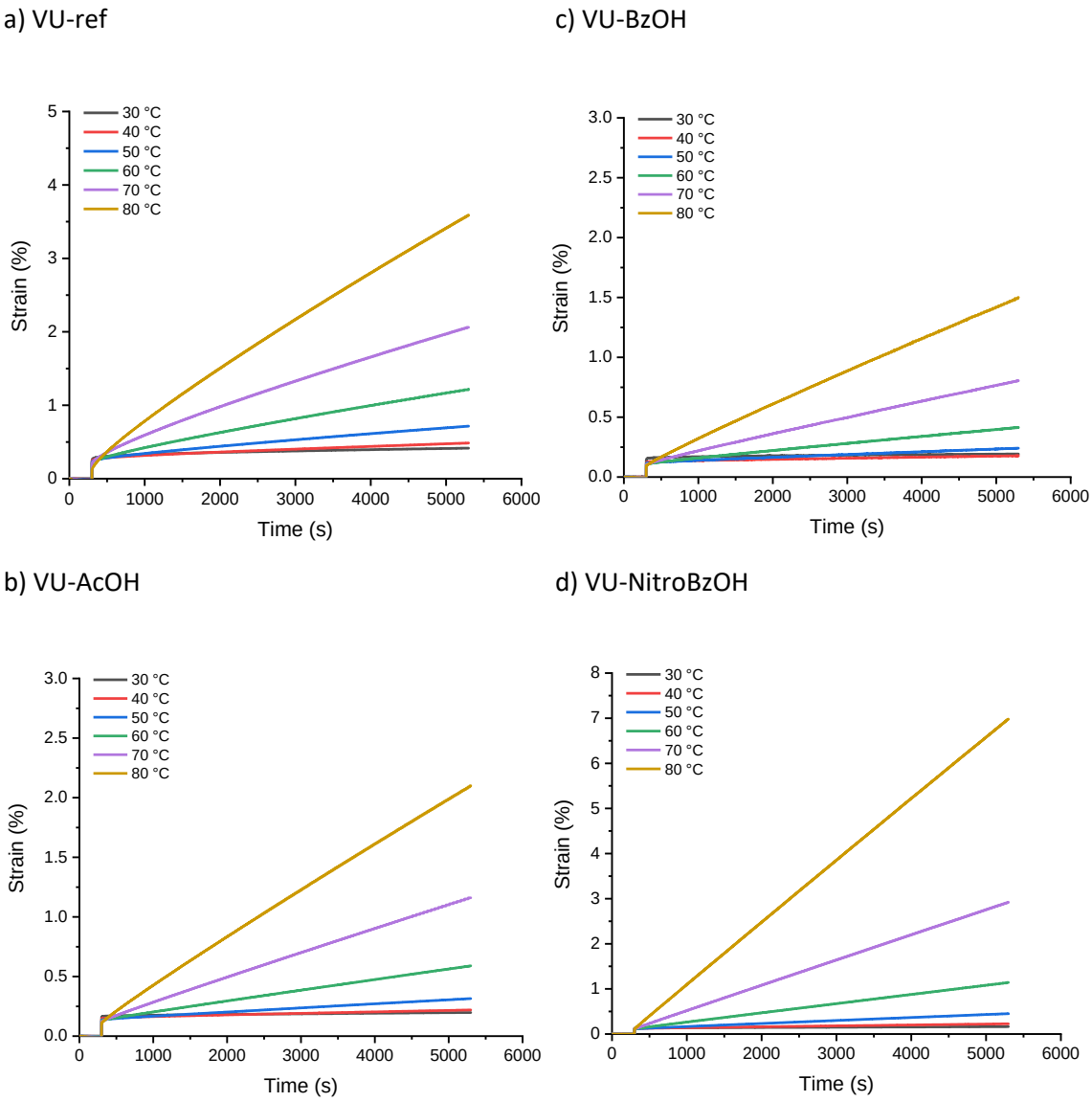

Figure S32. *Creep experiments of a) VU-ref, b) VU-AcOH, c) VU-BzOH and d) VU-NitroBzOH measured from 30 to 80 °C with a shear stress of 2 kPa.*

a) VU-AminoBzOH b) VU-AdamOHexcess

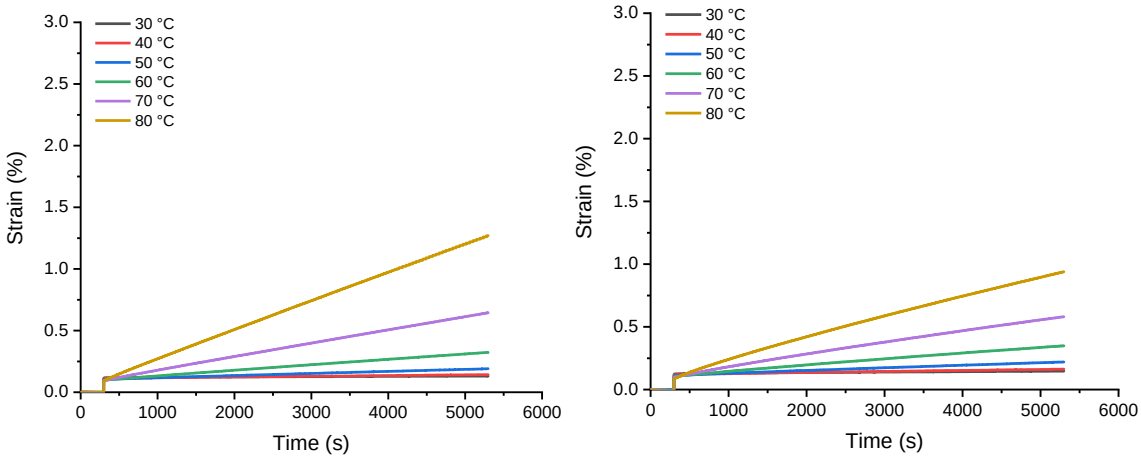

Figure S33. *Creep experiments of a) VU-AminoBzOH and b) VU-AdamOHexcess measured from 30 to 80 °C with a shear stress of 2 kPa.*

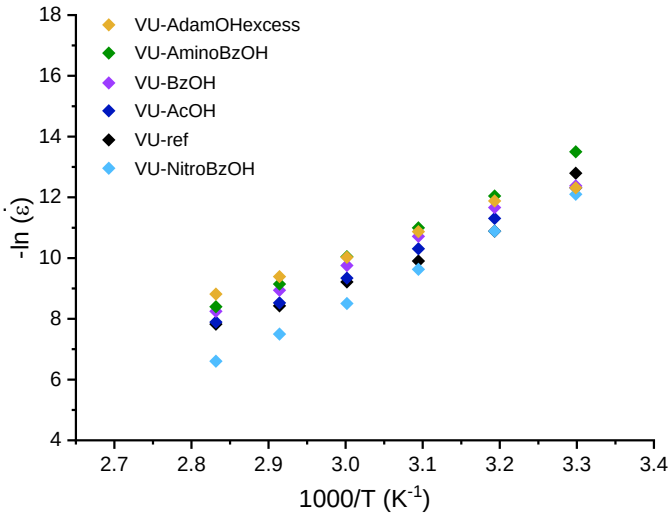

Figure S34. *Arrhenius plot based on creep rate values obtained by fitting the steady-state regime of the measured creep curves to a linear equation for VU-ref, VU-AcOH, VU-BzOH, VU-NitroBzOH, VU-AminoBzOH and VU-AdamOHexcess from 30 to 80 °C.*

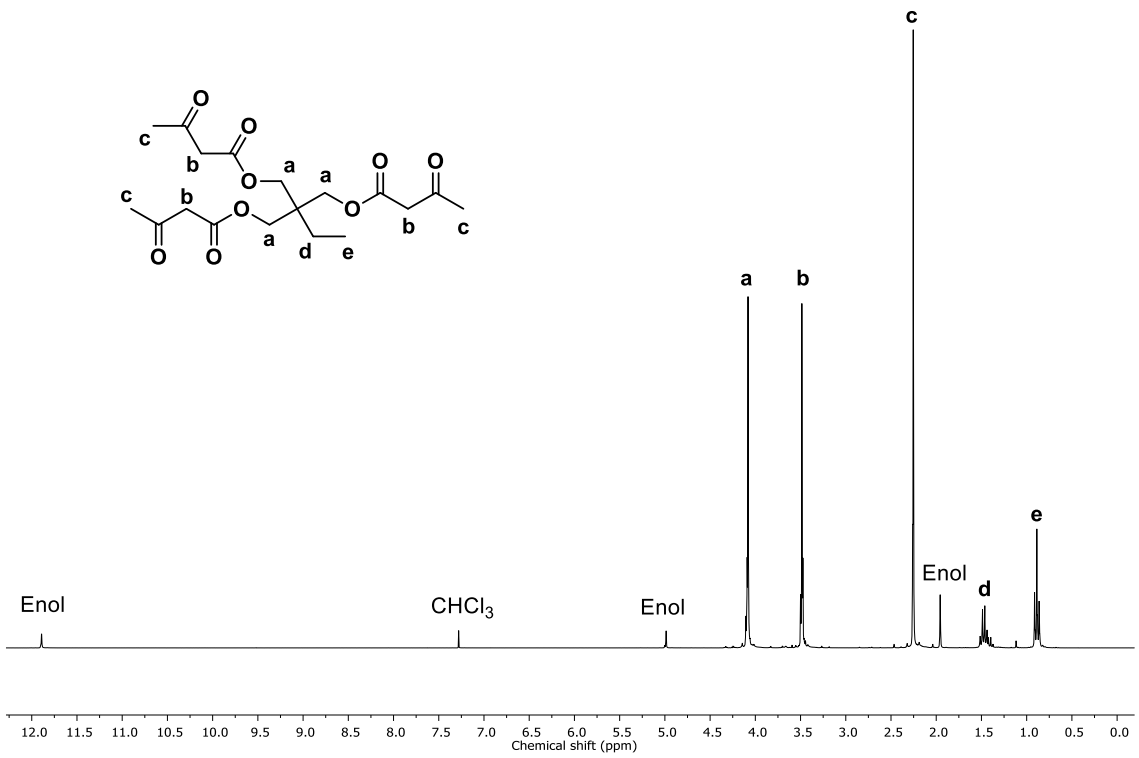

***Figure S35**. ^{1}H NMR of 1,1,1-trimethyl-propane trisacetoacetate in $CDCl_3$.*